Contributions of hydrophobic domain interface interactions to the folding and stability of human γD-crystallin

SHANNON L. FLAUGH, MELISSA S. KOSINSKI-COLLINS, AND JONATHAN KING
Department of Biology, Massachusetts Institute of Technology, Cambridge, Massachusetts 02139, USA
(RECEIVED September 9, 2004; FINAL REVISION November 24, 2004; ACCEPTED November 25, 2004)

Abstract

Human γD-crystallin (HγD-Crys) is a monomeric eye lens protein composed of two highly homologous β-sheet domains. The domains interact through interdomain side chain contacts forming two structurally distinct regions, a central hydrophobic cluster and peripheral residues. The hydrophobic cluster contains Met43, Phe56, and Ile81 from the N-terminal domain (N-td) and Val132, Leu145, and Val170 from the C-terminal domain (C-td). Equilibrium unfolding/refolding of wild-type HγD-Crys in guanidine hydrochloride (GuHCl) was best fit to a three-state model with transition midpoints of 2.2 and 2.8 M GuHCl. The two transitions likely corresponded to sequential unfolding/refolding of the N-td and the C-td. Previous kinetic experiments revealed that the C-td refolds more rapidly than the N-td. We constructed alanine substitutions of the hydrophobic interface residues to analyze their roles in folding and stability. After purification from *E. coli*, all mutant proteins adopted a native-like structure similar to wild type. The mutants F56A, I81A, V132A, and L145A had a destabilized N-td, causing greater population of the single folded domain intermediate. Compared to wild type, these mutants also had reduced rates for productive refolding of the N-td but not the C-td. These data suggest a refolding pathway where the domain interface residues of the refolded C-td act as a nucleating center for refolding of the N-td. Specificity of domain interface interactions is likely important for preventing incorrect associations in the high protein concentrations of the lens nucleus.

Keywords: human γD-crystallin; hydrophobic interactions; domain interface; partially folded intermediate; cataract; equilibrium unfolding/refolding transitions

The transparency of the human eye lens depends on the stability and solubility of the α-, β-, and γ-crystallin proteins (Delaye and Tardieu 1983; Fernald and Wright 1983). Crystallins are present in the enucleated fibrous lens cells at concentrations of 200–400 mg/mL, with the β- and γ-crystallins accounting for over 50% of the total protein (Oyster 1999). The β- and γ-crystallins are two domain proteins that structurally define the βγ-crystallin superfamily. The oligomeric α-crystallins exhibit in vitro molecular chaperone activity in addition to structural roles in lens transparency (Horwitz 1992; Boyle and Takemoto 1994). The crystallin proteins of the lens nucleus are synthesized early in lens development and do not regenerate during adulthood (Oyster 1999).

Human γD-crystallin (HγD-Crys) is a 173-amino-acid protein found in the densely packed lens nucleus. The crystal structure of HγD-Crys was recently solved to 1.25 Å (Fig. 1) and is consistent with the two-domain, primarily β-sheet structure of the βγ-crystallin superfamily (Basak et al. 2003). HγD-Crys is the third most abundant γ-crystallin in young human lenses (Lampi et al. 1997). Within each domain of HγD-Crys are two β-sheet Greek-key motifs. The domains are connected by an extended six-amino-acid

Reprint requests to: Jonathan King, Department of Biology, Massachusetts Institute of Technology, Building 68, Room 330, 31 Ames Street, Cambridge, MA 02139, USA; e-mail: jaking@mit.edu; fax: (617) 252-1843.

Article and publication are at http://www.proteinscience.org/cgi/doi/10.1110/ps.041111405.

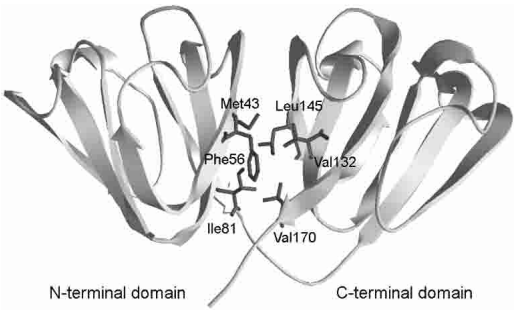

Figure 1. The crystal structure of wild-type HγD-Crys depicted in ribbon representation (Basak et al. 2003). Amino acids contributing to the hydrophobic cluster of the domain interface are shown in wire frame.

peptide and interact noncovalently through interdomain amino acid side chain contacts that form two structurally distinct regions. These are (1) a central hydrophobic cluster and (2) polar peripheral pairwise interactions surrounding the cluster. The hydrophobic cluster consists of Met43, Phe56, and Ile81 from the N-terminal domain (N-td) and Val132, Leu145, and Val170 from the C-terminal domain (C-td) (Fig. 1). Peripheral pairwise interactions are between Gln54/Gln143 and Arg79/Met147.

Mature-onset cataract is an exceptionally common protein deposition disease; it is the leading cause of blindness in the world and affects one in six people over age 40 in the U.S. (National Eye Institute 2002). Members of the α-, β-, and γ-crystallins have been recovered from the protein aggregates associated with mature-onset cataract (Hoenders and Bloemendal 1983). Single amino acid substitutions of HγD-Crys are associated with juvenile-onset congenital cataracts in humans (Heon et al. 1999; Santhiya et al. 2002). Many of these substitutions alter the surface properties of the molecule, which is thought to reduce phase transition barriers in situ (Pande et al. 2000, 2001).

The mechanisms of aggregation for many protein deposition diseases have been elucidated by studying the in vitro unfolding and refolding of their associated proteins (Westermark et al. 1990; DiFiglia et al. 1997). A common feature of these mechanisms is that the aggregation-prone species adopts a partially folded or nonnative conformation (Mitraki and King 1989; Wetzel 1994; Booth et al. 1997; Jiang et al. 2001; Nicholson et al. 2002). The processes that lead to loss of solubility and aggregation of crystallins are less well understood. In contrast to the aggregation mechanisms of some other protein deposition diseases, cataract is likely related to an unfolding and not a folding defect. The rare inherited juvenile-onset cataracts associated with mutations of HγD-Crys are caused by crystallization and intermolecular disulfide bonding of the native-state molecules (Pande et al. 2000, 2001). These mechanisms are unlikely to be related to those of mature-onset cataract. Instead, aggregation in the aged lens is probably correlated with destabilization of crystallin proteins. Covalent damage is profuse in the crystallins of aged and cataractous lenses, presumably resulting from a lifetime exposure to UV and oxidative stresses (Hoenders and Bloemendal 1983; Hanson et al. 1998, 2000). This damage may generate partially unfolded species of crystallins that polymerize through domain swapping, loop-sheet insertion, or another unknown mechanism. Though many of the damaged molecules may be bound by α-crystallin, this process appears to break down or become saturated in older adults.

Previous analysis of the unfolding and refolding of HγD-Crys in guanidine hydrochloride (GuHCl) identified an in vitro aggregation pathway that may provide a model of crystallin aggregation (Kosinski-Collins and King 2003). The aggregate formed from partially folded species after refolding to concentrations of GuHCl less than 1.0 M. The aggregated protein had ordered morphology resembling polymerized states of globular subunits as seen by atomic force microscopy (Kosinski-Collins and King 2003). Subsequent experiments determined that the C-td of HγD-Crys was more stable than the N-td and that the C-td acquired structure more rapidly during kinetic refolding (Kosinski-Collins et al. 2004). These results suggest that the domain interface of HγD-Crys may play a key role in folding and stability.

In this study we analyzed the role of the hydrophobic domain interface cluster in folding and stability. Single alanine substitutions of these residues were constructed, and the mutant proteins were analyzed for alterations in stability or refolding kinetics. The majority of the mutations affect both thermodynamic unfolding/refolding properties and kinetic refolding properties, suggesting that the hydrophobic cluster contributes to stability and acts as a nucleus for domain refolding.

Results

Protein expression and purification

Single alanine substitutions of the six hydrophobic domain interface residues of HγD-Crys were constructed using PCR-based primer extension. The mutant proteins were expressed at 37°C and purified by Ni-NTA affinity chromatography. Expression levels of all mutant proteins were comparable to wild type. The mutants behaved similarly to wild type during purification, and were present in the soluble fraction after cell lysis. All proteins purified to greater than 98% homogeneity as determined by SDS-PAGE (data not shown).

The proteins used in this study possessed an N-terminal His-tag of the sequence MKHHHHHHQ to aid in purification. Previous analysis of wild-type HγD-Crys with and without the His-tag confirmed that the exogenous peptide did not perceptibly alter the structure of the native state or the thermodynamic and kinetic unfolding/refolding proper-

ties (Kosinski-Collins and King 2003; Kosinski-Collins et al. 2004).

Circular dichroism and fluorescence spectroscopy

Circular dichroism (CD) and fluorescence emission spectroscopy were used to analyze the native state structures of hydrophobic domain interface mutants. The far-UV CD of wild-type HγD-Crys displayed a strong minimum at 218 nm in accord with previous results (Andley et al. 1996; Pande et al. 2000). All hydrophobic domain interface mutants had analogous spectra with a minimum at 218 nm, suggesting similar β-sheet content as wild type (Fig. 2). These results indicate that the overall secondary structure content of the mutant proteins was similar to wild-type HγD-Crys. Despite the fact that the structures of the mutant proteins appeared to be similar to wild type, dynamic properties of the proteins may have been altered. This phenomenon was previously observed in a mutational study of bovine pancreatic trypsin inhibitor (Beeser et al. 1997). The hydrophobic domain interface mutants could have had altered domain pairing not detected by far-UV CD. The near-UV CD spectra of wild-type HγD-Crys and all mutant proteins superimposed, suggesting similar aromatic environments (data not shown).

Fluorescence emission spectroscopy was used to further probe the environment of aromatic amino acids in wild-type and mutant HγD-Crys. HγD-Crys has four tryptophan residues, two per domain, buried in the hydrophobic cores of the two domains. Additionally, HγD-Crys has 14 tyrosines, many of which are surface-exposed. All fluorescence experiments performed here use an excitation wavelength of 295 nm to selectively excite the buried tryptophans and thus probe conformation of the domain cores. Wild-type HγD-Crys displayed a native-state emission maximum of 325 nm and an unfolded maximum of ~350 nm (Fig. 3). The fluorescence emission intensity increased upon unfolding, indicating that the tryptophans were quenched in the native fold (Fig. 3). This phenomenon was described previously for several of the β- and γ-crystallins (Kim et al. 2002; Bateman et al. 2003; Kosinski-Collins et al. 2004).

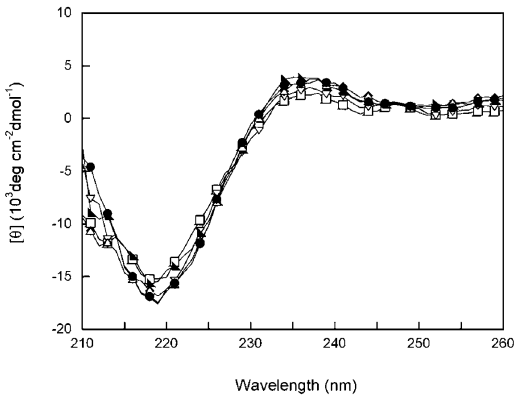

Figure 2. Far-UV CD of wild-type (◀), M43A (□), F56A (▼), I81A (▶), V132A (♦), L145A (△) and V170A (●) HγD-Crys. Samples contained 100 μg/mL protein in 10 mM sodium phosphate, 5 mM DTT, 1 mM EDTA (pH 7.0) at 37°C. A 0.25-cm pathlength cuvette was used for all measurements. All spectra were corrected for background buffer signal.

Tryptophan emission of domain interface mutants was measured in an analogous method as wild-type HγD-Crys. All mutant proteins displayed a native emission maximum of 325 nm and an unfolded maximum of ~350 nm (Fig. 3). Fluorescence emissions of all proteins were quenched in the native state (data not shown). These results suggest that the hydrophobic domain interface mutations did not disrupt the structure of the native-state buried hydrophobic cores. Similar to the CD measurements described above, tryptophan fluorescence of HγD-Crys would not report altered domain pairing.

Equilibrium unfolding and refolding of wild type

In order to assess the stability of the wild-type and mutant proteins, equilibrium unfolding/refolding experiments were performed. Tryptophan emission was used to probe the conformation of the domains using GuHCl as a denaturant at 37°C (pH 7.0). To best assess the shape of the transitions, a ratio of fluorescence intensities at 360 and 320 nm (FI 360/320 nm) was plotted as a function of GuHCl concentration.

Equilibrium unfolding/refolding of wild-type HγD-Crys has been previously investigated (Kosinski-Collins and King 2003). The unfolding and refolding samples in this earlier investigation were allowed to equilibrate at 25°C or 37°C for 6 h prior to measuring fluorescence emission. The transitions were best fit to a two-state model for both temperatures. At 25°C the unfolding and refolding transitions exhibited significant hysteresis. The unfolding transition had a midpoint of 3.7 M GuHCl, while the refolding transition had a midpoint of 2.7 M GuHCl. In contrast, at 37°C the two transitions deviated only slightly and both had midpoints of ~2.7 M GuHCl (Kosinski-Collins and King 2003). These observations suggested that structural transformations were controlled by a high kinetic barrier. Given that the unfolding transition but not the refolding transition changed with temperature, the kinetically controlled step was likely on the unfolding pathway.

In order to test for the presence of a high kinetic barrier to unfolding, we extended the equilibration time for all unfolding and refolding samples to 24 h. No hysteresis was evident between the unfolding and refolding transitions of wild-type HγD-Crys at these extended equilibration times (Fig. 4). Additionally, the increased times caused a shift in the location of the unfolding transition only. This further confirms the presence of a high kinetic barrier during unfolding. The molecular basis of the hysteresis is a subject of current investigations.

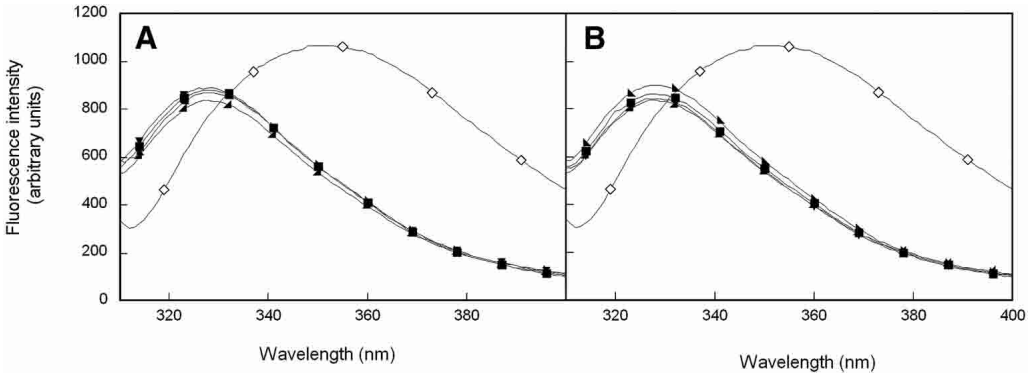

Figure 3. (*A*) Fluorescence spectroscopy of native (◀) and unfolded (◇) wild-type HγD-Crys, and native N-terminal domain mutants M43A (■), F56A (▼), and I81A (▶). (*B*) Fluorescence spectroscopy of native (◀) and unfolded (◇) wild-type HγD-Crys, and C-terminal domain mutants V132A (♦), L145A (▲), and V170A (●). Protein was present at 10 μg/mL protein in 10 mM sodium phosphate, 5 mM DTT, 1 mM EDTA (pH 7.0), and GuHCl where appropriate at 37°C. All spectra were corrected for background buffer signal.

Compared to the data collected with a 6-h equilibration time, the 24-h unfolding data exhibited a decreased slope in the transition region, possibly reflecting reduced cooperativity of the reaction. The m value for a two-state fit of 6-h data was 3.6 ± 0.1, while an m value of 2.7 ± 0.1 was calculated for a two-state fit of 24-h data. This change may suggest an unfolding/refolding mechanism for the 24-h data that is more complicated than the two-state model previously employed. To test this, equilibrium unfolding/refolding transitions of wild-type HγD-Crys were fit to both a two- and three-state model, and residuals of the fit were calculated (Fig. 4). The two-state model assumes direct transition between the native and unfolded states, while a three-state model allows for population of a partially folded intermediate. When fit to a two-state model the unfolding/refolding transitions had midpoints of 2.8 M GuHCl (Fig. 4A). By visual examination, the two-state fit appeared to be valid; however, the residuals displayed a semi-regular pat-

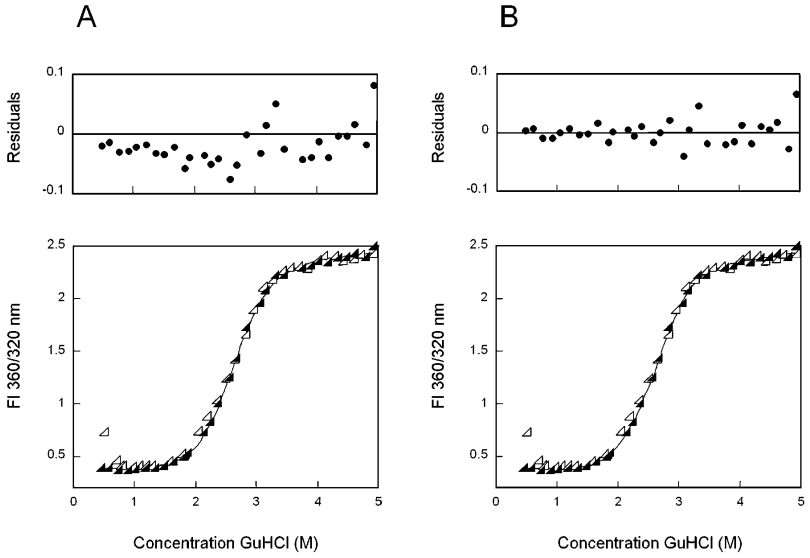

Figure 4. Equilibrium unfolding (closed symbols) and refolding (open symbols) of wild-type HγD-Crys in GuHCl probed by fluorescence emission. (*A*) The solid black line represents a two-state fit of equilibrium unfolding data. Residuals of the fit are shown. (*B*) Equilibrium unfolding data fit to a three-state model (solid black line), including residuals of the fit. Fluorescence spectra were recorded for each sample using an excitation wavelength of 295 nm. Fluorescence intensity at 360/320 nm was used in order to simultaneously monitor changes in the unfolding and native maxima. Samples were allowed to equilibrate in GuHCl at 37°C for 24 h prior to recording fluorescence emission spectra. By inspection, both fits appear suitable; however, residuals of the three-state fit are of lower magnitude and more random than those of the two-state fit. This observation along with other factors described in the text suggests that the three-state fit is a better description of the data.

tern, especially in the region of 2–3 M GuHCl (Fig. 4A). In contrast, fitting to a three-state model yielded a midpoint of 2.2 M for a transition from native to partially folded intermediate and a midpoint of 2.8 M GuHCl for an intermediate to unfolded transition (Fig. 4B). The residuals for the three-state fit had an overall lower magnitude and a more random arrangement than those of the two-state fit (Fig. 4B). This observation was reproducible in all three iterations of the experiment.

The three-state fit of the equilibrium unfolding data suggested that an intermediate was populated in the region of 2.3 M GuHCl. Given that the two-state fit was particularly poor in this region, it is likely that a three-state model is a better description of the data. The two transitions may correspond to independent unfolding/refolding of the two domains. These results along with apparent ΔG_{H2O} and m values calculated for the transitions are reported in Table 1.

In vitro aggregation

Consistent with previous results, wild-type HγD-Crys aggregated upon rapid refolding out of 5.5 M GuHCl (Kosinski-Collins and King 2003). A native-like conformation was attained when refolded to 1.0–1.8 M GuHCl. However, refolding to <1.0 M GuHCl resulted in the accumulation of a high-molecular weight aggregate. This was seen as a sharp increase in FI 360/320 nm due to right-angle light scattering by the aggregate (Fig. 4). Association by intermolecular disulfide bonding was prevented by inclusion of 5 mM DTT in all refolding samples.

Previous experiments investigated the morphology of the aggregate using atomic force microscopy. The aggregate adopted a fibrillar structure which did not bind Congo red or thioflavin T (Kosinski-Collins and King 2003). Previous results also indicate that the levels of aggregation are consistent over a range of incubation times from 3 to 41 h (Kosinski-Collins and King 2003). The levels of aggregation seen here with a 24-h incubation time were also consistent with those previously reported. Therefore, the effect of the increased incubation time was restricted to a change in the position of the unfolding transition.

All hydrophobic domain interface mutant chains also aggregated upon rapid refolding to less than 1.0 M GuHCl. As with wild type, a sharp increase in FI 360/320 nm values on equilibrium refolding traces was due to light scattering by the aggregate (Figs. 5, 6). Since the scattering would mask the presence of productively folded chains, the presence of native-like protein in aggregation samples was tested after centrifugation at 12,000 rpm. The soluble protein remaining after centrifugation displayed fluorescence emission spectra consistent with the native state spectra of the mutants (data not shown). Therefore, these mutant proteins exhibit partitioning between productive refolding and aggregation as previously described for wild type (Kosinski-Collins and King 2003).

Equilibrium unfolding and refolding of N-terminal domain mutants

The amino acids from the N-td that contribute to the interface hydrophobic cluster are Met43, Phe56, and Ile81 (Fig. 1). Equilibrium unfolding/refolding analyses of the single alanine substitution mutants of these residues were performed in a manner analogous to that used for wild-type HγD-Crys. It was possible to fit the equilibrium unfolding/refolding of M43A with both a two- and a three-state model (Fig. 5). The two-state fit yielded midpoints of 2.8 M GuHCl for both transitions. The three-state fit yielded midpoints of 2.2 M GuHCl for the first transition and 2.9 M GuHCl for the second transition (Table 1). Similar to wild-type HγD-Crys, the residuals of the three-state fit were more random and of lower magnitude, suggesting that the three-state model is a better representation of the data (data not shown). Assuming a three-state mechanism, the mutation had minimal effect on both the native to intermediate and intermediate to unfolded transitions.

Table 1. *Equilibrium unfolding/refolding parameters for wild-type and mutant HγD-Crys*

	Transition 1			Transition 2		
Protein	Apparent ΔG_{H2O}[a]	Apparent m value[b]	$[GuHCl]_{1/2}$[c]	Apparent ΔG_{H2O}[a]	Apparent m value[b]	$[GuHCl]_{1/2}$[c]
Wild type	7.7 ± 3%	3.6 ± 2%	2.2 ± 4%	8.9 ± 15%	3.1 ± 13%	2.8 ± 3%
M43A	7.7 ± 1%	3.7 ± 2%	2.2 ± 1%	8.1 ± 10%	2.8 ± 9%	2.9 ± 2%
F56A	6.1 ± 12%	3.9 ± 10%	1.6 ± 4%	9.3 ± 8%	3.2 ± 7%	2.9 ± 1%
I81A	5.3 ± 11%	3.7 ± 10%	1.5 ± 1%	8.7 ± 5%	3.0 ± 5%	2.9 ± 1%
V132A	5.0 ± 15%	3.7 ± 15%	1.3 ± 1%	7.8 ± 2%	3.1 ± 6%	2.5 ± 4%
L145A	6.5 ± 7%	3.9 ± 3%	1.6 ± 4%	7.5 ± 1%	2.9 ± 1%	2.6 ± 1%
V170A	N/A	N/A	N/A	10.2 ± 9%	4.0 ± 8%	2.5 ± 1%

[a] Free energy of unfolding in units of kcal*mol^{-1} calculated assuming a linear dependence on the concentration of GuHCl.
[b] m values in units of kcal*mol^{-1}*M^{-1}
[c] Transition midpoints in units of M.

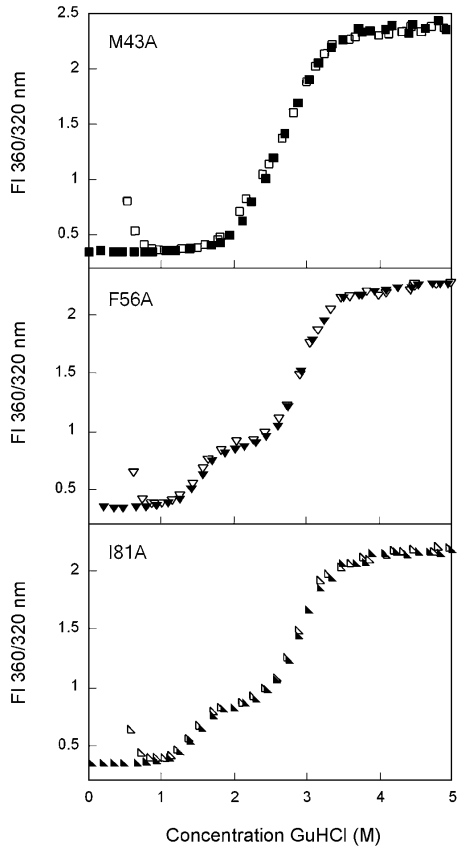

Figure 5. Equilibrium unfolding (closed symbols) and refolding (open symbols) of the N-terminal domain mutants M43A (■), F56A (▼), and I81A (▶) as probed by fluorescence emission. Protein was present at 10 μg/mL in 10 mM sodium phosphate, 5 mM DTT, 1 mM EDTA (pH 7.0), and GuHCl from 0 to 5.5 M. All samples were allowed to equilibrate for 24 h at 37°C before recording fluorescence emission. Data were analyzed by fluorescence intensity at 360/320 nm using an excitation wavelength of 295 nm. Transitions for all mutants were best fit by a three-state model.

The equilibrium unfolding/refolding transitions of F56A were significantly different from wild type (Fig. 5). A noticeable plateau was present in the transition region from ~2.0 to 2.3 M GuHCl, suggesting greater population of the partially folded intermediate. The intermediate species had a fluorescence signal that was distinct from that of the native and unfolded conformations (Fig. 5). Equilibrium unfolding/refolding data were best fit to a three-state model with transition midpoints of 1.6 and 2.9 M GuHCl for the first and second transitions, respectively (Table 1).

Similar to F56A, the mutant I81A also displayed a plateau from 2.0 to 2.3 M GuHCl where the fluorescence emission spectrum was different from both the native and unfolded states (Fig. 5). The unfolding/refolding transitions were best fit to a three-state model with a transition midpoint of 1.5 M GuHCl for the transition from native to intermediate and a midpoint of 2.9 M GuHCl for the intermediate to unfolded transition (Table 1).

Equilibrium unfolding and refolding of C-terminal domain mutants

The amino acids of the C-td that participate in the interface hydrophobic cluster are Val132, Leu145, and Val170 (Fig. 1). The mutant protein V132A displayed transitions similar to those described for F56A and I81A above (Fig. 6). The unfolding/refolding transitions were best fit to a three-state model with a partially folded intermediate populated in the region of 2.3 M GuHCl. A transition midpoint of 1.3 M GuHCl was calculated for the native to intermediate transition, and a midpoint of 2.5 M GuHCl was calculated for the intermediate to unfolded transitions (Table 1).

Equilibrium unfolding/refolding of L145A also displayed a three-state transition where the intermediate was populated at 2.3 M GuHCl (Fig. 6). The native to intermediate

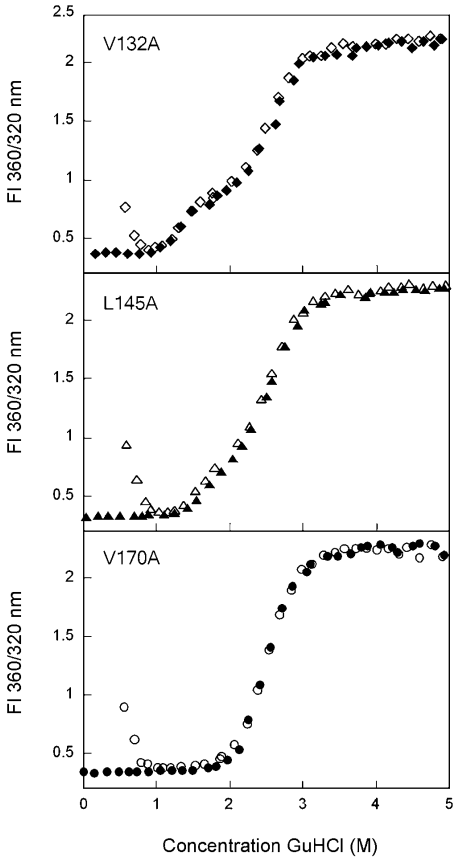

Figure 6. Equilibrium unfolding (closed symbols) and refolding (open symbols) of the C-terminal domain mutants V132A (♦), L145A (▲), and V170A (●). Fluorescence spectroscopy was used to probe the solvent accessibility of tryptophans in each sample using an excitation wavelength of 295 nm. Data were analyzed by fluorescence intensity at 360/320 nm. Protein was present at 10 μg/mL in 10 mM sodium phosphate, 5 mM DTT, 1 mM EDTA (pH 7.0), and GuHCl from 0 to 5.5 M. Samples were incubated at 37°C for 24 h prior to measuring fluorescence emission. Transitions of all mutants, except V170A, were best fit by a three-state model. The transitions of V170A were best fit by a two-state model.

transition had a midpoint of 1.6 M GuHCl, and the intermediate to unfolded transition had a midpoint of 2.6 M GuHCl (Table 1). The partially folded intermediate had a unique fluorescence spectrum similar to the intermediate conformation populated by all other domain interface mutants (data not shown).

The equilibrium unfolding/refolding transitions of V170A were best fit to a two-state transition with a random pattern of residuals (Fig. 6). The two transitions overlaid identically and displayed transition midpoints of 2.5 M GuHCl (Table 1). Unlike wild type and M43A, it was not possible to fit the transitions of V170A to a three-state model. However, it is not possible to rule out a three-state mechanism based on this observation alone. Further analysis will be performed to elucidate the unfolding/refolding mechanism of this mutant.

Productive refolding kinetics of wild type

In order to assess the role of hydrophobic domain interface residues in kinetic refolding, structural transformations of the mutant proteins were monitored over time using fluorescence as a probe of conformation. To allow for comparison, these experiments were performed similarly to our previous analyses of kinetic refolding of HγD-Crys (Kosinski-Collins et al. 2004). Unfolded proteins were diluted from 5.5 to 1.0 M GuHCl, and the decrease in fluorescence intensity at 350 nm was monitored to follow burial of tryptophan residues. A syringe injection port was used instead of a stopped-flow apparatus, since the major structural transformations of HγD-Crys occur on a second timescale (Kosinski-Collins et al. 2004). These experiments did not address folding intermediates that may have been populated on a subsecond timescale.

Previous analysis of wild-type HγD-Crys showed that refolding kinetics were best fit to two exponentials, suggesting that an intermediate was populated on the kinetic refolding pathway (Kosinski-Collins and King 2003; Kosinski-Collins et al. 2004). The partially folded intermediate was more fluorescent than the native state and less fluorescent than the unfolded state at 350 nm. The transition from unfolded to intermediate occurred with a half-time ($t_{1/2}$) of 15 sec, and the transition from intermediate to native occurred with a $t_{1/2}$ of 190 sec (Kosinski-Collins et al. 2004).

Triple-tryptophan mutant proteins were used to further analyze the structural transformations corresponding to the two kinetic fits of wild-type HγD-Crys (Kosinski-Collins et al. 2004). As mentioned previously, wild-type HγD-Crys has four intrinsic tryptophans, two per domain, buried in the hydrophobic cores. Triple-tryptophan mutants were constructed where three of the endogenous tryptophans were substituted with phenylalanines. The four mutant proteins retained one endogenous tryptophan so that unfolding/refolding of the N-td and C-td could be followed independently of each other. This technique has been employed to elucidate the folding pathways of cellular retinoic acid binding protein I and phosphoglycerate kinase (Beechem et al. 1995; Sherman et al. 1995; Clark et al. 1998).

Kinetic refolding of mutant proteins retaining a tryptophan in the C-td were best fit to a three-state model (two exponentials) with $t_{1/2}$ values of 30 sec for the first transition and 150–300 sec for the second transition. In contrast, kinetic refolding of mutant proteins retaining a tryptophan in the N-td were best fit to a two-state model with $t_{1/2}$ values of ~200 sec. These data suggest that tryptophans in the C-td were buried first, followed by burial of tryptophans in the N-td.

Productive refolding experiments of wild-type HγD-Crys were repeated here to ensure that the measurements were comparable to those reported previously. Kinetic refolding of wild type was best fit by two exponentials where a partially folded intermediate (I) was populated on the productive refolding pathway (Figs. 7, 8).

$$\text{Denatured} \xrightarrow{k_1} [\text{I}] \xrightarrow{k_2} \text{Native}$$

In excellent agreement with previous results, a $t_{1/2}$ of 15 sec was calculated for the transition from unfolded to intermediate, and a $t_{1/2}$ of 190 sec was calculated for the transition

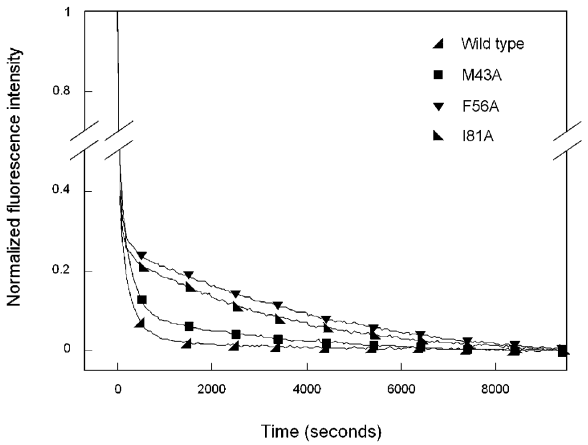

Figure 7. Productive kinetic refolding of wild-type (◀) HγD-Crys and N-terminal domain mutants M43A (■), F56A (▼), and I81A (▶). Black lines represent data points taken every 1 sec, with symbols included for ease of viewing. Fluorescence emissions were normalized for ease of viewing and comparison. Wild-type and mutants proteins were initially unfolded for 3 h at a concentration of 100 μg/mL in 5.5 M GuHCl, 37°C. Refolding was initiated by dilution of unfolded proteins into 10 mM sodium phosphate, 5 mM DTT, and 1 mM EDTA (pH 7.0), using a syringe injection port. The final concentration of GuHCl in refolding samples was 1.0 M, and the final protein concentration was 10 μg/mL. The temperature was maintained at 37°C during refolding using a circulating water bath. Refolding was monitored by changes in fluorescence emission at 350 nm for 3 h. The data were fit to two exponentials to calculate rate constants. Fits were improved by inclusion of additional exponentials; however, it was unclear whether these additional variables actually represented population of further intermediates.

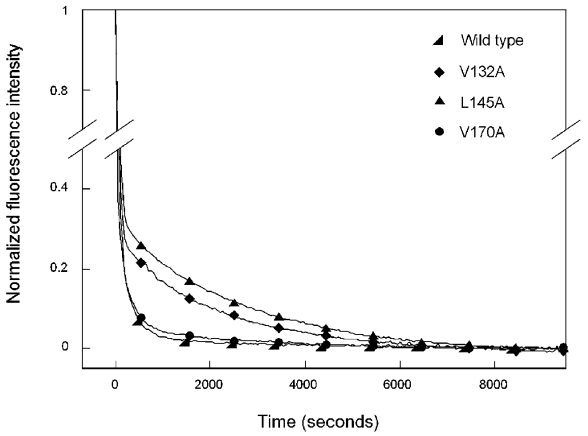

Figure 8. Productive kinetic refolding of wild type (◀) HγD-Crys and C-terminal domain mutants V132A (◆), L145A (▲), and V170A (●). Black lines represent data points taken every 1 sec, with symbols included for ease of viewing. Fluorescence emissions were normalized for ease of viewing and comparison. The proteins were first unfolded at 100 μg/mL in 5.5 M GuHCl, 37°C for 3 h. Refolding was initiated by dilution of unfolded proteins into 10 mM sodium phosphate, 5 mM DTT, and 1 mM EDTA (pH 7.0), using a syringe injection port, to give a final concentration of 1.0 M GuHCl and 10 μg/mL protein. Structural changes during refolding were monitored by changes in fluorescence emission at 350 nm for 3 h. The temperature was maintained at 37°C during refolding using a circulating water bath. The data were fit to two exponentials to calculate rate constants. Inclusion of extra exponentials improved the fits. It was not possible to determine whether the extra exponentials characterized the genuine population of further intermediates.

from intermediate to native (Kosinski-Collins et al. 2004). The kinetic refolding parameters calculated for wild-type and mutant HγD-Crys are reported in Table 2.

Productive kinetic refolding experiments were performed on interface mutants in a manner analogous to that described for wild-type HγD-Crys. Kinetic refolding curves for all mutant proteins were best fit to two exponentials. The kinetic fits in the early part of the curve were not particularly good (data not shown). While the fits were improved with the inclusion of additional exponentials, it was unclear whether these additional variables represented actual intermediates or were due to experimental, instrumental, or human error. From the triple-tryptophan studies, the spectroscopic changes during kinetic refolding of wild-type HγD-Crys were shown to correspond to sequential domain refolding (Kosinski-Collins et al. 2003). Since fitting the data to two exponentials yielded phases that could be defined in terms of major structural transformations, discussion of the refolding kinetics has been limited to these clearly defined intermediates.

Table 2. *Kinetic refolding parameters for wild-type and mutant HγD-Crys*

Protein	k_1 (sec^{-1})	$t_{1/2}$ (sec)	k_2 (sec^{-1})	$t_{1/2}$ (sec)
Wild type	0.048 ± 1%	15 ± 1%	0.0037 ± 3%	190 ± 3%
M43A	0.009 ± 10%	79 ± 10%	0.0004 ± 1%	1700 ± 1%
F56A	0.030 ± 6%	23 ± 6%	0.0002 ± 12%	2700 ± 12%
I81A	0.034 ± 4%	21 ± 4%	0.0003 ± 4%	2100 ± 4%
V132A	0.016 ± 13%	45 ± 13%	0.0005 ± 6%	1400 ± 6%
L145A	0.014 ± 9%	52 ± 9%	0.0004 ± 15%	1600 ± 15%
V170A	0.018 ± 2%	38 ± 2%	0.0026 ± 16%	300 ± 16%

Productive refolding kinetics of N-terminal domain mutants

Kinetic refolding of the mutant protein M43A was best fit by a three-state model (two exponentials), suggesting the population of a partially folded intermediate similar to wild type (Fig. 7). Upon dilution out of GuHCl, the fluorescence intensity of M43A at 350 nm rapidly decreased with a $t_{1/2}$ of 79 sec (Table 1). This change presumably corresponded to a transition from the unfolded to intermediate state. The $t_{1/2}$ value for M43A was less than that calculated for the first transition of wild-type HγD-Crys. After the initial phase, a slower decrease in fluorescence was observed with a $t_{1/2}$ of 1700 sec. This loss of fluorescence correlated with a transition from the intermediate to the native state. The $t_{1/2}$ value for M43A differed by an order of magnitude from that calculated for the second transition of wild type.

Kinetic refolding of F56A was also best fit by a three-state model. An initial rapid decrease in fluorescence intensity with a $t_{1/2}$ of 23 sec was followed by a slower decrease in fluorescence with a $t_{1/2}$ of 2700 sec (Fig. 7). By inspection, the transition from unfolded to intermediate for F56A was indistinguishable from that of wild type and had a $t_{1/2}$ value similar to that calculated for wild type. In contrast, the second transition from intermediate to native did not overlay with wild type and had a $t_{1/2}$ value more than 14 times greater.

I81A also underwent kinetic refolding that was best described by two exponentials. An initial rapid decrease in fluorescence occurred with a $t_{1/2}$ of 21 sec and was followed by a slower phase that occurred with a $t_{1/2}$ of 2100 sec (Fig. 7). Similar to the results described for M43A and F56A, the transition from unfolded to intermediate was indistinguishable from wild type, while the rate of transition from intermediate to native was significantly reduced.

Productive refolding kinetics of C-terminal domain mutants

Productive refolding kinetics of the mutant protein V132A were best fit to a three-state model (Fig. 8). The initial rapid decrease in fluorescence occurred with a $t_{1/2}$ of 45 sec (Table 2). This value differs slightly from that calculated for wild-type HγD-Crys but is still within the same order of magnitude. In contrast, the rate of transition from interme-

diate to native was greatly reduced compared to that of wild type. The second transition of V132A occurred with a $t_{1/2}$ of 1400 sec (Table 2).

Kinetic refolding of L145A proceeded in a manner identically to that described for V132A and was best fit to a three-state model (Fig. 8). The first transition had a $t_{1/2}$ of 52 sec and the second transition a $t_{1/2}$ of 1600 sec. The $t_{1/2}$ value for unfolded to intermediate was similar to that for wild type, while the $t_{1/2}$ value for intermediate to native was appreciably larger (Table 2).

Of all mutants examined here, refolding kinetics of V170A were the most similar to those of wild-type HγD-Crys. Changes in fluorescence intensity at 350 nm during refolding overlaid that of wild type very closely (Fig. 8). The initial transformation from unfolded to intermediate occurred with a $t_{1/2}$ of 38 sec, and the second transition to native occurred with a $t_{1/2}$ of 300 sec (Table 2).

Discussion

HγD-Crys is a two-domain protein of the eye lens that must remain stable for an entire human lifetime without the possibility of regeneration. Along with other lens crystallins, HγD-Crys is found in the insoluble aggregates associated with mature-onset cataract. HγD-Crys is composed of two domains that share ~34% sequence identity and adopt highly similar, primarily β-sheet folds (Fig. 1). The two-domain nature of HγD-Crys and the other β- and γ-crystallins is hypothesized to have arisen from a gene duplication event (Wistow et al. 1983).

The domains of HγD-Crys interact noncovalently through interdomain side chain contacts forming two structurally distinct regions (Basak et al. 2003). These are a highly conserved hydrophobic cluster of Met43, Phe56, Ile81, Val132, Leu145, and Val170 and polar peripheral pairwise interactions between Gln54/Gln143 and Arg79/Met147 (Fig. 1). The domain interface of HγD-Crys is relatively similar in amino acid composition to domain interfaces of other proteins. Overall, the amino acid composition of domain interfaces more closely resembles that of protein surfaces rather than protein cores (Jones et al. 2000). However, hydrophobic residues are still highly prevalent in both inter- and intrachain domain interactions (Jones et al. 2000).

Differential domain stability of the β- and γ-crystallins

Many of the β- and γ-crystallins studied to date exhibit differential domain stability. Bovine γB-crystallin (BγB-Crys) displayed a three-state transition in urea at pH 2.0 and 20°C (Mayr et al. 1997). At pH 2.0, the isolated N-td of BγB-Crys was much more stable than the C-td, presumably due to the abundance of positively charged residues on the surface of the C-td at this acidic pH. At pH 7.0 the domains had similar stabilities, and equilibrium unfolding of the full-length protein was two-state (Mayr et al. 1997). Bovine βB2-crystallin also displayed differential domain stability (Wieligmann et al. 1999). The crystal structure of βB2-crystallin is a domain-swapped dimer where the N-td of one monomer pairs with the C-td of the other (Bax et al. 1990). The isolated C-td of bovine βB2-crystallin was significantly more stable than the isolated N-td (Wieligmann et al. 1999).

Studies of triple-tryptophan mutants of HγD-Crys suggest that the C-td is more stable than the N-td (Kosinski-Collins et al. 2004). The transition midpoint of proteins retaining tryptophans in the N-td was 1.3 M GuHCl, whereas the midpoint of mutants retaining tryptophans in the C-td was 2.0 M GuHCl. These data suggest that an intermediate would be populated during equilibrium unfolding/refolding of the wild-type protein. Previous analyses using an incubation time of 6 h could not distinguish a three-state transition for wild-type HγD-Crys (Kosinski-Collins and King 2003; Kosinski-Collins et al. 2004). In the experiments described here, the incubation time was increased to 24 h, which altered the equilibrium transition and eliminated the unfolding/refolding hysteresis (Fig. 4). At these extended equilibration times, the transition had reduced cooperativity, which may reflect a more complex transition such as would be expected for a three-state mechanism. When fit to a three-state model, the first transition had a midpoint of 2.2 M GuHCl and the second transition a midpoint of 2.8 M GuHCl. Overall, the three-state model was a better description of the data than the two-state model, especially in the region of 2–3 M GuHCl. From these observations, we hypothesize that wild-type HγD-Crys populates a partially folded intermediate in equilibrium unfolding/refolding experiments at ~2.3 M GuHCl. The stabilities of the domains elucidated by triple-tryptophan mutants, we suggest that these two transitions correspond to unfolding/refolding of the N-td (at lower concentrations of GuHCl) and the C-td (at high concentrations of GuHCl). The transition midpoints of triple-tryptophan mutant proteins were considerably lower than these values, potentially due to destabilizing effects of the triple mutations.

Domain interface interactions are crucial for stability

Contribution of domain interface interactions to the stability of BγB-Crys has been previously studied (Palme et al. 1997, 1998). The domain interface of BγB-Crys is comprised of a central hydrophobic cluster including a phenylalanine at position 56 and peripheral pairwise interactions (Wistow et al. 1983). Palme et al. (1997, 1998) mutated Phe56 to alanine, aspartate, or tryptophan and analyzed the effects on the structure and stability of BγB-Crys in urea at pH 2.0 and 20°C. All proteins displayed reduced stability of the C-td that varied with the mutation. Substitution with aspartate or alanine resulted in considerable destabilization,

whereas substitution with tryptophan had less of an affect (Palme et al. 1997). Domain core structures of the mutants were indistinguishable from the wild-type protein, and local structure around residue 56 was unchanged (Palme et al. 1998). These results suggest that, despite the destabilizing effects, the global structure of BγB-Crys was too rigid to adjust to the altered size or hydrophobicity of the mutations.

Similar to the results described above for BγB-Crys, the hydrophobic domain interface residues of HγD-Crys are also critical for stability. All mutants except V170A were best fit to a three-state model where the first transitions likely corresponded to unfolding/refolding of the N-td and the second transition to unfolding/refolding of the C-td. According to this hypothesis, C-td unfolding/refolding for the mutants F56A, I81A, V132A, and L145A occurred with a midpoint between 2.5 and 2.9 M GuHCl. These values are relatively similar to that calculated for the second transition of wild type (2.8 M GuHCl), further supporting a three-state mechanism for the wild-type protein. Substitution of Met43, Phe56, and Ile81 from the N-td resulted in an increased midpoint of 2.9 M GuHCl for transitions of the C-td. If the intermediate had a folded C-td and unfolded N-td as hypothesized, interface residues from the N-td would not be expected to stabilize the intermediate. Increased stability of the intermediate as is seen with M43A, F56A, and I81A may be due to a favorable decrease in solvent-exposed hydrophobics compared to wild type because of the alanine substitutions. In contrast, mutation of Val132 and Leu145 resulted in decreased stability of the intermediate. The domain interface of the C-td is likely structured in the intermediate conformation. Consequently, mutations that disrupt correct intradomain hydrophobic packing would be expected to decrease stability of the intermediate.

In contrast to the marginal affect on stability of the C-td, the N-td was significantly destabilized by mutations of Phe56, Ile81, Val131, and Leu145. For these mutants, unfolding/refolding of the N-td occurred with a midpoint between 1.3 and 1.6 M GuHCl (Table 1). These values were significantly lower than that calculated for the first transition of wild type when fit to a three-state model (2.2 M GuHCl). Therefore, mutation of residues located in the C-td affected stability of the N-td but not vice versa. From these results we postulate that the stability of the N-td is dependent on correct domain interface contacts, while stability of the C-td is not enhanced by domain pairing. Destabilization of the N-td resulted in population of the intermediate over a greater range of GuHCl concentrations than was seen for the wild-type protein.

Mutation of Met43 and Val170 had significantly different effects on the stability of HγD-Crys. The equilibrium unfolding/refolding transitions of M43A did not differ dramatically from wild type, and had ΔG_{H2O}, m values, and transition midpoints very similar to those of wild type. In contrast, the transitions of V170A were best fit to a two-state model with midpoints of 2.5 M GuHCl. This may suggest that unfolding/refolding of V170A occurs by a direct transition between the native and unfolded states. An alternative interpretation is that the mutant did unfold/refold by a three-state mechanism, but that the two transitions were not discernible. This may have been caused by a shift of the first transition to higher concentrations of GuHCl, or shift of the second transition to lower concentrations of GuHCl. One of these phenomena or a combination of the two would effectively merge the transitions. From comparison to the transitions of wild type, we suspect that mutation of Val170 had both effects described above. That is, the first transition was stabilized relative to wild type and the second transition was destabilized relative to wild type. Further experiments will be done to determine which if either of these hypotheses can explain these data.

Kinetic refolding pathway of HγD-Crys

We previously studied the productive refolding pathway of HγD-Crys using triple-tryptophan mutant proteins (Kosinski-Collins et al. 2004). Previous investigations of the β- and γ-crystallins analyzed behavior of the domains by studying polypeptides that corresponded to isolated N- and C-td's of the proteins (Sharma et al. 1990; Mayr et al. 1994; Wieligmann et al. 1999; Wenk et al. 2000). This approach does not reveal properties of the domains in context of the full-length proteins. This limitation has been circumvented in our analysis of triple-tryptophan mutants, since we were able to independently follow folding of the two domains while still maintaining a full-length protein.

During kinetic refolding of HγD-Crys, the tryptophans of the C-td were buried before those of the N-td (Kosinski-Collins et al. 2004). These results suggest a productive refolding pathway where the C-td refolds first followed by the N-td. Given that the domain interface of HγD-Crys does not contain any fluorescent amino acids, it was not possible to determine when the domain interface became structured in these experiments.

Three simple models are illustrated in Figure 9 to describe the role of domain interface residues in the sequential domain refolding pathway of HγD-Crys. In the first model, the domain interface residues initially collapse and form a nucleating center for refolding of the C-td and subsequently the N-td. If HγD-Crys refolded by this first pathway, domain interface mutations would be expected to decrease the refolding rates for both the C-td and the N-td. In the second model, the two domains refold independently and subsequently come together to form interface contacts. Mutations of domain interface residues would likely not reduce refolding rates of the N-td or the C-td in this model. In the third model, the C-td refolds first and the interface amino acids of the C-td act as a nucleating center for refolding of the N-td. By this model, mutations of domain interface residues

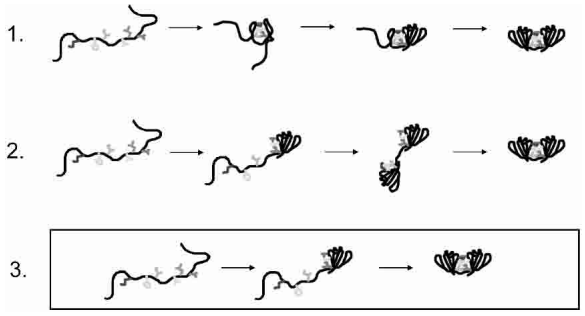

Figure 9. Schematic diagram of three models to describe the role of the domain interface during sequential domain refolding of wild-type HγD-Crys. Model 3 was consistent with the data presented here. The C-td of HγD-Crys refolded first, resulting in an intermediate that had an unpaired, solvent-exposed domain interface. This surface likely acted as a nucleating center for refolding of the N-td.

would likely result in decreased rates for refolding of the N-td only.

Kinetic refolding of all interface mutants was best fit to a three-state model similar to wild type. Comparing these data to the triple-tryptophan mutant data, it was possible to correlate the two transitions to sequential refolding of the C-td and N-td (Kosinski-Collins et al. 2004). Assuming that the domains of the mutant proteins refolded in the same order as wild type, the mutants M43A, F56A, I81A, V132A, and L145A all had similar $t_{1/2}$ values for refolding of the C-td but greatly increased $t_{1/2}$ values for refolding of the N-td. These results suggested a productive refolding pathway consistent with the third model described above, in which the interface residues of the refolded C-td act as a nucleating center for refolding of the N-td (Fig. 9).

From the perspective of in vitro domain folding, a sequential nucleation-based folding pathway as was exhibited by HγD-Crys may be considered detrimental for productive folding. This is because sequential domain folding results in an increased lifetime of partially folded intermediates that may partition into kinetically trapped aggregates (Jaenicke 1999). The single folded domain conformer populated during equilibrium and kinetic unfolding/refolding experiments is an attractive target for the aggregation-prone species in the in vitro aggregation pathway of HγD-Crys (Kosinski-Collins and King 2003; Kosinski-Collins et al. 2004).

Implications for understanding stability and oligomerization in the lens

In this investigation the hydrophobic domain interface residues were substituted with alanine, resulting in a loss of hydrophobic surface area. If residues of the cluster contributed uniformly to stability by hydrophobic burial, differences in effects of the mutations would be expected to correlate with buried accessible surface area of the wild-type residue (Rose et al. 1985; Zhou and Zhou 2004). Greater accessible surface area was buried for Phe56 than Val132, but the mutant protein V132A was more destabilized than the mutant F56A. This indicates that the locations of the hydrophobic domain interface residues are important in determining their role in stability and folding of HγD-Crys. This may reflect different packing densities around the residues. Additionally, unique identity and position of domain interface residues are thought to be important in determining the oligomeric states of the β- and γ-crystallins (Hope et al. 1994; Mayr et al. 1994; Trinkl et al. 1994).

The two-domain β- and γ-crystallins comprise over 50% of the protein in the lens nucleus and adopt highly similar domain topology with domain interactions that are predominated by a central hydrophobic cluster (Lapatto et al. 1991; Slingsby et al. 1997; Oyster 1999). Protein concentration in the lens nucleus is extremely high (200–400 mg/mL), necessitating precise control of folding and oligomerization in order to prevent aberrant intermolecular associations. Due to the hydrophobic nature of the domain interfaces and the ability of β- and γ-crystallins to adopt single folded domain conformers, the domain interfaces may be regions of the molecules that are particularly prone to incorrect protein-protein interactions. Given these factors, it is reasonable to assume that the β- and γ-crystallins may have evolved for specificity of domain interface residues in folding, stability, and oligomerization in order to prevent incorrect domain interactions in the crowded lens nucleus.

Aggregation and cataract

It is currently unknown which conformations of crystallin proteins are the aggregation-prone species that lead to cataract. Crystallins in the lens nucleus are subject to a lifetime of oxidative and radiative stress. The crystallin proteins of both young and old lenses are covalently damaged as a result of these insults (Hoenders and Bloemendal 1983; Hanson et al. 1998, 2000). Covalent damage may result in destabilization and partial unfolding into the aggregation-prone species that are precursors to cataract formation. These partially folded species may be sequestered by α-crystallin in order to prevent aggregation. In fact, it has been shown that partially structured conformations of β- and γ-crystallins are capable of binding to α-crystallin in vitro as a result of mutation or after exposure to heat (Lampi et al. 2002; Liang 2004; Sathish et al. 2004). We are currently testing whether α-crystallin is able to bind the single folded domain conformer of HγD-Crys described here. The age-onset nature of noncongenital forms of cataract may reflect accumulation of sufficient levels of damage to induce unfolding or saturation of α-crystallin.

Materials and methods

Mutagenesis, expression, and purification of recombinant HγD-Crys

Alanine substitutions of residues Met43, Phe56, Ile81, Val132, Leu145, and Val170 were constructed using PCR-based site-directed mutagenesis. Primers encoding the site-specific alanine substitutions (IDT-DNA) were used to amplify a pQE.1 plasmid encoding the HγD-Crys gene with an N-terminal 6-His tag (Kosinski-Collins et al. 2004). All resulting plasmids were sequenced to verify the substitutions and to ensure that no additional mutations were present (Massachusetts General Hospital).

Recombinant wild-type and mutant HγD-Crys proteins were expressed and purified as described by Kosinski-Collins et al. (2004). Briefly, proteins were expressed in *Escherichia coli*, and cell lysates were purified to over 98% homogeneity by affinity chromatography with a Ni-NTA resin (QIAGEN).

Circular dichroism spectroscopy

CD spectra of the purified proteins were collected with an AVIV model 202 CD spectrometer. Proteins were present in concentrations of 100 μg/mL for far-UV CD and 300 μg/mL for near-UV CD. Protein concentrations were determined by absorbance at 280 nm using an extinction coefficient of 41,040 cm^{-1} M^{-1} for wild-type and mutant His-tagged proteins. All samples contained 10 mM sodium phosphate, 5 mM DTT, 1 mM EDTA (pH 7.0). The buffer signal was subtracted from all spectra. Spectra were collected from 200 to 260 nm to monitor secondary structure and from 260 to 340 nm to monitor tertiary structure. An internal Peltier thermo-electric temperature controller was used to maintain the temperature at 37°C.

Fluorescence emission spectroscopy

Fluorescence emission spectra were recorded with a Hitachi F-4500 fluorimeter. Intrinsic tryptophan fluorescence was measured using an excitation wavelength of 295 nm and monitoring emission from 310 to 400 nm. A slitwidth of 10 nm was used for both excitation and emission. All samples contained 10 μg/mL purified protein in 10 mM sodium phosphate, 5 mM DTT, 1 mM EDTA (pH 7.0), and 5.5 M GuHCl where appropriate. Emission spectra were corrected for the buffer signal. A circulating water bath was used to maintain the temperature at 37°C.

Equilibrium unfolding and refolding

Equilibrium unfolding experiments were performed by diluting purified proteins to 10 μg/mL in 0 to 5.5 M GuHCl (purchased as an 8.0 M solution from Sigma-Aldrich). All unfolding samples contained 10 mM sodium phosphate, 5 mM DTT, and 1 mM EDTA (pH 7.0). Unfolding samples were incubated at 37°C for 24 h to ensure equilibrium had been reached.

Equilibrium refolding experiments were carried out by initially preparing unfolded stock solutions of 100 μg/mL purified protein in 5.5 M GuHCl. The unfolded stock solutions were incubated at 37°C for 5 h. The unfolded stocks were then diluted into refolding samples to give a final protein concentration of 10 μg/mL. Refolding samples contained 10 mM sodium phosphate, 5 mM DTT, 1 mM EDTA (pH 7.0), and GuHCl from 0.55 to 5.5 M. The refolding samples were allowed to reach equilibrium by incubation at 37°C for 24 h.

Fluorescence emission spectra were recorded for each unfolding and refolding sample using a Hitachi F-4500 fluorimeter as described above. The concentration of GuHCl in the unfolding/refolding samples was determined by measuring the refractive index. Data were analyzed by plotting the concentration of GuHCl for each sample versus the ratio of fluorescence intensities at 360 and 320 nm (FI 360/320 nm). All data were plotted from 0 to 5.0 M GuHCl instead of 5.5 M GuHCl to improve visual clarity of the transitions. Equilibrium unfolding/refolding experiments of the wild-type and mutant proteins were performed three times each.

Equilibrium unfolding and refolding data were fit to a two-state model by the methods of Greene and Pace (1974) or a three-state model by the methods of Clark et al. (1993) using the curve-fitting feature of Kaleidagraph (Synergy software). The model that best fit the data was selected based on a random distribution of residuals. Transition midpoints, ΔG_{H2O}, and m values were calculated for all transitions from these fits.

Productive refolding kinetics

Kinetic refolding experiments were carried out by diluting purified proteins to 100 μg/mL in 5.5 M GuHCl. The solutions were unfolded by incubation at 37°C for 5 h. Refolding buffer containing 10 mM sodium phosphate, 5 mM DTT, and 1 mM EDTA (pH 7.0) was equilibrated to 37°C with stirring. Fluorescence emission of the refolding buffer was continually monitored in a Hitachi F-4500 fluorimeter using an excitation wavelength of 295 nm and an emission wavelength of 350 nm. Unfolded stocks were diluted into the refolding buffer using a syringe port injection system to give a final protein concentration of 10 μg/mL in 1.0 M GuHCl. Fluorescence emission of the refolding sample was monitored at 350 nm for 3 h. The fluorescence emission spectra of resulting refolded samples were measured to ensure that the proteins had refolded into a native-like conformation. Kinetic refolding data were fit to one, two, and three exponentials using the curve-fitting feature of Kaleidagraph. The model with the best fit was determined by inspection. Kinetic refolding experiments of the wild-type and mutant proteins were performed two times each.

Acknowledgments

We thank Ishara Mills and Veronica Zepeda for helpful discussions. This work was supported by NIH grant GM17980 to J.K. S.F. was supported by a Cleo and Paul Schimmel Fellowship.

References

Andley, U.P., Mathur, S., Griest, T.A., and Petrash, J.M. 1996. Cloning, expression, and chaperone-like activity of human αA-crystallin. *J. Biol. Chem.* **271:** 31973–31980.

Basak, A., Bateman, O., Slingsby, C., Pande, A., Asherie, N., Ogun, O., Benedek, G.B., and Pande, J. 2003. High-resolution X-ray crystal structures of human γD crystallin (1.25Å) and the R58H mutant (1.15Å) associated with aculeiform cataract. *J. Mol. Biol.* **328:** 1137–1147.

Bateman, O.A., Sarra, R., van Genesen, S.T., Kappe, G., Lubsen, N.H., and Slingsby, C. 2003. The stability of human acidic β-crystallin oligomers and hetero-oligomers. *Exp. Eye Res.* **77:** 409–422.

Bax, B., Lapatto, R., Nalini, V., Driessen, H., Lindley, P.F., Mahadevan, D., Blundell, T.L., and Slingsby, C. 1990. X-ray analysis of β B2-crystallin and evolution of oligomeric lens proteins. *Nature* **347:** 776–780.

Beechem, J.M., Sherman, M.A., and Mas, M.T. 1995. Sequential domain unfolding in phosphoglycerate kinase: Fluorescence intensity and anisotropy

stopped-flow kinetics of several tryptophan mutants. *Biochemistry* **34:** 13943–13948.
Beeser, S.A., Goldenberg, D.P., and Oas, T.G. 1997. Enhanced protein flexibility caused by a destabilizing amino acid replacement in BPTI. *J. Mol. Biol.* **269:** 154–164.
Booth, D.R., Sunde, M., Bellotti, V., Robinson, C.V., Hutchinson, W.L., Fraser, P.E., Hawkins, P.N., Dobson, C.M., Radford, S.E., Blake, C.C., et al. 1997. Instability, unfolding and aggregation of human lysozyme variants underlying amyloid fibrillogenesis. *Nature* **385:** 787–793.
Boyle, D. and Takemoto, L. 1994. Characterization of the α-γ and α-β complex: Evidence for an in vivo functional role of α-crystallin as a molecular chaperone. *Exp. Eye Res.* **58:** 9–15.
Clark, A.C., Sinclair, J.F., and Baldwin, T.O. 1993. Folding of bacterial luciferase involves a non-native heterodimeric intermediate in equilibrium with the native enzyme and the unfolded subunits. *J. Biol. Chem.* **268:** 10773–10779.
Clark, P.L., Weston, B.F., and Gierasch, L.M. 1998. Probing the folding pathway of a β-clam protein with single-tryptophan constructs. *Fold Des.* **3:** 401–412.
Delaye, M. and Tardieu, A. 1983. Short-range order of crystallin proteins accounts for eye lens transparency. *Nature* **302:** 415–417.
DiFiglia, M., Sapp, E., Chase, K.O., Davies, S.W., Bates, G.P., Vonsattel, J.P., and Aronin, N. 1997. Aggregation of huntingtin in neuronal intranuclear inclusions and dystrophic neurites in brain. *Science* **277:** 1990–1993.
Fernald, R.D. and Wright, S.E. 1983. Maintenance of optical quality during crystalline lens growth. *Nature* **301:** 618–620.
Greene Jr., R.F. and Pace, C.N. 1974. Urea and guanidine hydrochloride denaturation of ribonuclease, lysozyme, α-chymotrypsin, and β-lactoglobulin. *J. Biol. Chem.* **249:** 5388–5393.
Hanson, S.R., Smith, D.L., and Smith, J.B. 1998. Deamidation and disulfide bonding in human lens γ-crystallins. *Exp. Eye Res.* **67:** 301–312.
Hanson, S.R., Hasan, A., Smith, D.L., and Smith, J.B. 2000. The major in vivo modifications of the human water-insoluble lens crystallins are disulfide bonds, deamidation, methionine oxidation and backbone cleavage. *Exp. Eye Res.* **71:** 195–207.
Heon, E., Priston, M., Schorderet, D.F., Billingsley, G.D., Girard, P.O., Lubsen, N., and Munier, F.L. 1999. The γ-crystallins and human cataracts: A puzzle made clearer. *Am. J. Hum. Genet.* **65:** 1261–1267.
Hoenders, H.J. and Bloemendal, H. 1983. Lens proteins and aging. *J. Gerontol.* **38:** 278–286.
Hope, J.N., Chen, H.C., and Hejtmancik, J.F. 1994. Aggregation of β A3-crystallin is independent of the specific sequence of the domain connecting peptide. *J. Biol. Chem.* **269:** 21141–21145.
Horwitz, J. 1992. α-crystallin can function as a molecular chaperone. *Proc. Natl. Acad. Sci.* **89:** 10449–10453.
Jaenicke, R. 1999. Stability and folding of domain proteins. *Prog. Biophys. Mol. Biol.* **71:** 155–241.
Jiang, X., Smith, C.S., Petrassi, H.M., Hammarstrom, P., White, J.T., Sacchettini, J.C., and Kelly, J.W. 2001. An engineered transthyretin monomer that is nonamyloidogenic, unless it is partially denatured. *Biochemistry* **40:** 11442–11452.
Jones, S., Marin, A., and Thornton, J.M. 2000. Protein domain interfaces: Characterization and comparison with oligomeric protein interfaces. *Protein Eng.* **13:** 77–82.
Kim, Y.H., Kapfer, D.M., Boekhorst, J., Lubsen, N.H., Bachinger, H.P., Shearer, T.R., David, L.L., Feix, J.B., and Lampi, K.J. 2002. Deamidation, but not truncation, decreases the urea stability of a lens structural protein, βB1-crystallin. *Biochemistry* **41:** 14076–14084.
Kosinski-Collins, M.S. and King, J. 2003. In vitro unfolding, refolding, and polymerization of human γD crystallin, a protein involved in cataract formation. *Protein Sci.* **12:** 480–490.
Kosinski-Collins, M.S., Flaugh, S.L., and King, J. 2004. Probing folding and fluorescence quenching in human γD crystallin Greek key domains using triple tryptophan mutant proteins. *Protein Sci.* **13:** 2223–2235.
Lampi, K.J., Ma, Z., Shih, M., Shearer, T.R., Smith, J.B., Smith, D.L., and David, L.L. 1997. Sequence analysis of βA3, βB3, and βA4 crystallins completes the identification of the major proteins in the young human lens. *J. Biol. Chem.* **272:** 2268–2275.
Lampi, K.J., Kim, Y.H., Bachinger, H.P., Boswell, B.A., Lindner, R.A., Carver, J.A., Shearer, T.R., David, L.L., and Kapfer, D.M. 2002. Decreased heat stability and increased chaperone requirement of modified human βB1-crystallins. *Mol. Vis.* **8:** 359–366.
Lapatto, R., Nalini, V., Bax, B., Driessen, H., Lindley, P.F., Blundell, T.L., and Slingsby, C. 1991. High resolution structure of an oligomeric eye lens β-crystallin. Loops, arches, linkers and interfaces in β B2 dimer compared to a monomeric γ-crystallin. *J. Mol. Biol.* **222:** 1067–1083.
Liang, J.J. 2004. Interactions and chaperone function of αA-crystallin with T5P γC-crystallin mutant. *Protein Sci.* **13:** 2476–2482.
Mayr, E.M., Jaenicke, R., and Glockshuber, R. 1994. Domain interactions and connecting peptides in lens crystallins. *J. Mol. Biol.* **235:** 84–88.
———. 1997. The domains in γB-crystallin: Identical fold-different stabilities. *J. Mol. Biol.* **269:** 260–269.
Mitraki, A. and King, J. 1989. Protein folding intermediates and inclusion body formation. *Biotechnology* **7:** 690–697.
National Eye Institute (U.S.) 2002. "Vision problems in the U.S." Prevent Blindness in America, Bethesda, MD.
Nicholson, E.M., Mo, H., Prusiner, S.B., Cohen, F.E., and Marqusee, S. 2002. Differences between the prion protein and its homolog Doppel: A partially structured state with implications for scrapie formation. *J. Mol. Biol.* **316:** 807–815.
Oyster, C.W. 1999. *The human eye: Structure and function.,* Chap. 12. Sinauer Associates, Inc., Sunderland, MA.
Palme, S., Slingsby, C., and Jaenicke, R. 1997. Mutational analysis of hydrophobic domain interactions in γB-crystallin from bovine eye lens. *Protein Sci.* **6:** 1529–1536.
Palme, S., Jaenicke, R., and Slingsby, C. 1998. X-ray structures of three interface mutants of γB-crystallin from bovine eye lens. *Protein Sci.* **7:** 611–618.
Pande, A., Pande, J., Asherie, N., Lomakin, A., Ogun, O., King, J.A., Lubsen, N.H., Walton, D., and Benedek, G.B. 2000. Molecular basis of a progressive juvenile-onset hereditary cataract. *Proc. Natl. Acad. Sci.* **97:** 1993–1998.
Pande, A., Pande, J., Asherie, N., Lomakin, A., Ogun, O., King, J., and Benedek, G.B. 2001. Crystal cataracts: Human genetic cataract caused by protein crystallization. *Proc. Natl. Acad. Sci.* **98:** 6116–6120.
Rose, G.D., Geselowitz, A.R., Lesser, G.J., Lee, R.H., and Zehfus, M.H. 1985. Hydrophobicity of amino acid residues in globular proteins. *Science* **229:** 834–838.
Santhiya, S.T., Shyam Manohar, M., Rawlley, D., Vijayalakshmi, P., Namperumalsamy, P., Gopinath, P.M., Loster, J., and Graw, J. 2002. Novel mutations in the γ-crystallin genes cause autosomal dominant congenital cataracts. *J. Med. Genet.* **39:** 352–358.
Sathish, H.A., Koteiche, H.A., and McHaourab, H.S. 2004. Binding of destabilized βB2-crystallin mutants to α-crystallin: The role of a folding intermediate. *J. Biol. Chem.* **279:** 16425–16432.
Sharma, A.K., Minke-Gogl, V., Gohl, P., Siebendritt, R., Jaenicke, R., and Rudolph, R. 1990. Limited proteolysis of γ II-crystallin from calf eye lens. Physicochemical studies on the N-terminal domain and the intact two-domain protein. *Eur. J. Biochem.* **194:** 603–609.
Sherman, M.A., Beechem, J.M., and Mas, M.T. 1995. Probing intradomain and interdomain conformational changes during equilibrium unfolding of phosphoglycerate kinase: Fluorescence and circular dichroism study of tryptophan mutants. *Biochemistry* **34:** 13934–13942.
Slingsby, C., Norledge, B., Simpson, A., Bateman, O.A., Wright, G., Driessen, H.P.C., Lindley, P.F., Moss, D.S., and Bax, B. 1997. X-ray diffraction and structure of crystallins. *Prog. Ret. and Eye Res.* **16:** 3–29.
Trinkl, S., Glockshuber, R., and Jaenicke, R. 1994. Dimerization of β B2-crystallin: The role of the linker peptide and the N- and C-terminal extensions. *Protein Sci.* **3:** 1392–1400.
Wenk, M., Herbst, R., Hoeger, D., Kretschmar, M., Lubsen, N.H., and Jaenicke, R. 2000. γ S-crystallin of bovine and human eye lens: Solution structure, stability and folding of the intact two-domain protein and its separate domains. *Biophys. Chem.* **86:** 95–108.
Westermark, P., Sletten, K., Johansson, B., and Cornwell 3rd, G.G. 1990. Fibril in senile systemic amyloidosis is derived from normal transthyretin. *Proc. Natl. Acad. Sci.* **87:** 2843–2845.
Wetzel, R. 1994. Mutations and off-pathway aggregation of proteins. *Trends Biotechnol.* **12:** 193–198.
Wieligmann, K., Mayr, E.M., and Jaenicke, R. 1999. Folding and self-assembly of the domains of βB2-crystallin from rat eye lens. *J. Mol. Biol.* **286:** 989–994.
Wistow, G., Turnell, B., Summers, L., Slingsby, C., Moss, D., Miller, L., Lindley, P., and Blundell, T. 1983. X-ray analysis of the eye lens protein γ-II crystallin at 1.9Å resolution. *J. Mol. Biol.* **170:** 175–202.
Zhou, H. and Zhou, Y. 2004. Quantifying the effect of burial of amino acid residues on protein stability. *Proteins* **54:** 315–322.